| 1 | Martínez, M., Shearer, C.S. and Brearley, A.J. (2023) Epitaxial fluorapatite veins in Northwest Africa 99 host apatite: Clues on the geochemistry of late hydrothermal fluids on Mars. Meteoritics and Planeta | | |
|----------------|--|--|--|
| 2 | Science (https://doi.org/10.1111/maps.14042 | | |
| 3 | | | |
| 4 | | | |
| 5 | | | |
| 6 | Epitaxial fluorapatite vein in Northwest Africa 998 host apatite: | | |
| 7 | Clues on the geochemistry of late hydrothermal fluids on Mars | | |
| 8 | | | |
| 9 | Marina Martínez ^{a*,†} , Charles K. Shearer ^{a,b} , and Adrian J. Brearley ^a | | |
| 10 | | | |
| 11 | ^a Department of Earth & Planetary Sciences, MSC03-2040, 1University of New Mexico, | | |
| 12 | Albuquerque, NM 87131, USA (mmartinezjimenez@unm.edu) | | |
| 13 | ^b Institute of Meteoritics, MSC03-2040, University of New Mexico, Albuquerque, NM 87131, | | |
| 14 | USA | | |
| 15 | | | |
| 16 | | | |
| 17 | | | |
| 18 | | | |
| 19 | | | |
| 20 | | | |
| 21 | | | |
| 22 | | | |
| 23 24 25 | *Corresponding author. †Present address: Universitat Autònoma de Barcelona (UAB), Edifici Cs, Av. de l'Eix Central, s/n, 08193 Cerdanyola del Vallès, Barcelona (Marina.Martinez@uab.cat) | | |

ABSTRACT

| Secondary minerals in martian nakhlites provide a powerful tool for investigating the | | | | |
|--|--|--|--|--|
| nature, composition, and duration of aqueous activity in the martian crust. Northwest Africa | | | | |
| (NWA) 998 crystallized early from the nakhlite magmatic source and has evidence of minimal | | | | |
| signatures of the late hydrothermal alteration event that altered the nakhlites. Using FIB-TEM | | | | |
| techniques to study a cumulus apatite grain in NWA 998, we report the first evidence of a | | | | |
| submicron-scale vein consisting of fluorapatite and a SiO2-rich phase. Fluorapatite grew | | | | |
| epitaxially on the walls of an opened cleavage plane of host F-bearing chlorapatite and the SiO ₂ - | | | | |
| rich phase filled the center of the vein. The presence of nano-porosity and nanometer-scale | | | | |
| amorphous material, and the sharp interface between the vein and the host apatite indicate the | | | | |
| vein represents a coupled dissolution-reprecipitation process that generated apatite of a different | | | | |
| composition that was more stable with the fluid. Using experimental data from Kusebauch et al. | | | | |
| (2015) and the diffusion coefficients of Cl in apatite following the method of Li et al. (2020), we | | | | |
| conclude that the vein was caused by a low temperature (~300°C), slightly acidic, F-,Si-rich, | | | | |
| aqueous fluid that acted as a closed system. Based on the characteristics of vein (formation by | | | | |
| rapid injection of fluid) and the fluid (composition, temperature, pH), and lack of terrestrial | | | | |
| weathering products in our SEM and TEM images, we infer that the vein is pre-terrestrial in | | | | |
| origin. Our observations support the hypothesis that the heat source triggering a hydrothermal | | | | |
| system was a low-shock velocity impact and rule out a magmatic origin. Finally, the vein could | | | | |
| have formed from a late-stage fluid different from that reported in other nakhlites, but formation | | | | |
| during the same magmatic event by, for example, a less evolved fluid, might also be plausible. | | | | |
| Keywords: nakhlites, apatite, epitaxial vein, hydrothermal system, Mars | | | | |

Introduction

The nakhlites are cumulus igneous rocks from Mars that crystallized from basaltic magmas at relatively low pressures ~1.3 Ga ago (Harvey and McSween, 1992; Nyquist et al., 2001; Swindle and Olson, 2004; Treiman, 2005; Beck et al., 2006; Mikouchi et al., 2012). The chemical and isotopic characteristics of the nakhlites show evidence of mixing with a volatilerich crustal component (i.e., a fluid) that assimilated into the nakhlite melt (e.g., McCubbin et al., 2013; Shearer et al., 2018; Martínez et al., 2023a). The nakhlites are clinopyroxenites with cumulus augite and less abundant cumulus olivine, with variable amounts of mesostasis, interstitial regions to cumulus grains that contain minor phases, including silicates (e.g., plagioclase, alkali-feldspar, and silica), oxides (titanomagnetite, ilmenite), sulfides (troilite, pyrrhotite, chalcopyrite), and phosphates (apatite), among others (e.g., Harvey and McSween, 1992; Wadhwa and Crozaz, 1995; Treiman, 2005). The nakhlites also exhibit a wide range of secondary minerals, including silicates (smectite clays), carbonates (siderite), oxides, hydroxides, halides, and sulfates (e.g., Gooding et al., 1991; Treiman, 1993; Bridges and Grady, 1999, 2000; Gillet et al., 2002; Changela and Bridges, 2011; Cartwright et al., 2013), suggestive of a later aqueous alteration episode and thus, serve to understand the interaction between groundwater and igneous rocks. These secondary minerals are typically found as veins in olivine and mesostasis regions (e.g., Bridges and Grady, 2000; Hallis and Taylor, 2011; Lee et al., 2015a,b; Cao et al., 2022), although fluid inclusions trapped along fractures within augite grains have also been recognized (e.g., Bridges et al., 2000; Hallis and Lee, 2014). The absence of crosscutting veins in the nakhlites and the truncation of these veins by fusion crusts that formed during entry into the Earth's atmosphere suggest that the nakhlites experienced only one single hydrothermal event, and that the alteration event is pre-

terrestrial in origin (Gooding et al., 1991). Noble gas (K-Ar) and Rb-Sr measurements of

49

50

51

52

53

54

55

56

57

58

59

60

61

62

63

64

65

66

67

68

69

70

"iddingsite" veins in the nakhlites constrain the timing of this alteration event to 633 ± 23 Ma (Swindle et al., 2000; Borg and Drake, 2005). Therefore, the nakhlites offer a unique opportunity to learn about the interactions between the lithosphere (Amazonian volcanic terranes), hydrosphere, and atmosphere from a recent geologic time.

Based on veins within brittle fractures, the requirement for a rapidly cooled heat source, and the relatively low peak-shock pressures that the nakhlites have experienced (20 GPa, Nyquist et al., 2001), Changela and Bridges (2010) argued that the altering hydrothermal system recorded in the nakhlites originated at the margin of an impact crater. The fluid source is thought to originate close to Lafayette and then migrated upwards (Changela and Bridges, 2010), because aqueous alteration signatures are most significant in this sample (Treiman, 2005).

Within the 18 nakhlites known to date (10 unpaired), NWA 998 represents the bottom of the cumulus pile (deepest crystallization), with the slowest cooling rate (i.e., chemical equilibration of olivine and completely crystalline mesostasis with blocky plagioclase), containing large augite crystals that are normally zoned to pigeonite rims (e.g., Treiman, 2005; Treiman and Irving, 2008). NWA 998 and Lafayette are the only two nakhlites that contain cumulus orthopyroxene (Treiman, 2005), and NWA 998 possibly contains cumulus apatite (McCubbin et al., 2013; Martínez et al., 2023b). NWA 998 appears to be the least aqueously altered nakhlite. Pre-terrestrial, secondary mineral assemblages in NWA 998 have only been identified as minor "iddingsite" veins in olivine (Treiman and Irving, 2008). However, Breton (2017) also identified a rare alteration product (enriched in Fe and Mn and depleted in Si) found along the margins of the alteration veins, and possible desiccation cracks, cross-cutting the Sirich ('iddingsite') veins, although the grain size was too small to resolve at SEM scales.

Apatite textures and compositions in the nakhlites have been used to reconstruct their magmatic and subsolidus histories and to better understand volatile reservoirs, their interactions, and their behavior in the martian crust and mantle (e.g., Treiman and Irving, 2008; McCubbin et al., 2013). Specifically, apatite in NWA 998 reflects a complex record of both magmatic and subsolidus processes and extracting petrogenetic and volatile records are difficult and fraught with interpretive issues. For these reasons, examining apatite at the nanometer scale provides valuable insights into the complex thermal, geochemical, and fluid evolution history (Martínez et al., 2023a,b).

In the present study, we have investigated the occurrence of veins within a cumulus apatite grain by TEM. The goals of our study are to: (1) evaluate the possible processes that could have formed the vein (terrestrial versus martian), (2) acquire new information on the nature of the ephemeral water-rich environment that existed in the recent past in the subsurface of Mars, (3) determine the potential role that hydrothermal systems played in the volatile evolution of nakhlites and on the planet, and (4) evaluate how the post-magmatic history affects the utilization of apatite to reconstruct the magmatic and volatile behavior of the Martian mantle.

Samples and analytical methods

A polished 1-inch round petrographic thin section of Northwest Africa 998 (,002) from the meteorite collection of Institute of Meteoritics Collection at the University of New Mexico was used for this study. After being coated with a 10 nm layer of carbon, the thin section was studied to identify and locate apatite grains using backscattered electron (BSE) imaging and energy dispersive spectroscopy (EDS) X-ray analysis on a FEI Quanta 3D Dualbeam® field emission gun (FEG) SEM/FIB. The analytical conditions used were 30 kV accelerating voltage and a beam current of 4 nA. The instrument is equipped with an EDAX Genesis EDS system and

an Apollo 40 SDD 40 mm² EDS detector for qualitative X-ray analysis. BSE imaging at very low kV (5 kV) and high contrast were performed to examine apatite grains at high magnifications and determine their possible microstructures and petrographic occurrences, such as veins.

117

118

119

120

121

122

123

124

125

126

127

128

129

130

131

132

133

134

135

136

137

138

139

A focused ion beam (FIB) sample for transmission electron microscopy (TEM) of the selected apatite grain was prepared using the FEI Quanta 3D FEGSEM/FIB instrument. The region of interest was protected from sputtering by the Ga⁺ ion beam by depositing a 2 µm-thick Pt strip across the area prior to sample extraction. The TEM sample was removed from the thin section by the in situ lift-out technique using an Omniprobe 200 micromanipulator and transferred onto Cu half grids. The sample was then ion milled to a thickness of approximately 50 nm for optimal high-resolution imaging with ion beam currents decreasing from 1 nA down to 53 pA for the final stage of ion milling, at 30 kV operating voltage. A final, low-angle polishing step with a 2 kV and 50 pA ion beam was carried out to remove any possible sputtered material. Bright-field (BF) TEM imaging, high-resolution TEM (HR-TEM), scanning TEM/TEM-EDS, selected area electron diffraction (SAED), high-angle annular dark field (HAADF) STEM imaging, STEM-EDS X-ray mapping, and X-ray intensity line profiles were performed on the FIB samples using a JEOL 2010F FEG TEM/scanning TEM (STEM) operating at 200 kV and JEOL NEOARM 200CF Aberration Corrected Scanning Transmission Electron Microscope. The STEM and TEM images were acquired and processed using GATAN Microscopy Suite® (GMS) software. On the JEOL 2010F, quantitative EDS analyses were obtained in both STEM and TEM modes using an Oxford AZTec X-ray analysis system with a X-Max 80N 80 mm² SDD energy dispersive X-ray spectrometer (EDS) detector system. Quantitative EDS data in the vein were obtained over areas of 100 x 400 nm for 500 sec (STEM)

and using a spot size of 5 to minimize beam damage, and areas of a few microns (i.e., 2-3 µm) in the host apatite for 300 seconds (TEM). On the JEOL NEOARM, EDS line profiles across the vein were obtained using dual 100 mm² JEOL EDS detectors interfaced to an Oxford Instruments AZTec X-ray analysis system and software. STEM-EDS data were collected using a 200 pA beam current. Quantification of EDS data was conducted using the Cliff-Lorimer thin film approximation with theoretical k-factors. Errors were all <5% (relative error). The analyses assume oxygen present according to oxide stoichiometry and normalized to 100 wt%. All SEM and TEM studies were performed at the Department of Earth and Planetary Science at the University of New Mexico.

Results

General characteristics of the host apatite

A completed BSE mosaic of the studied thin section of NWA 998 and the petrographic characteristics of the apatite grains are described in Martínez et al. (2023a). Northwest Africa 998 is the only nakhlite known to contain cumulus apatite and thus, apatites in this sample are the largest among the nakhlites, ranging from ~50 to ~200 μm in size (Fig. 1). Cumulus apatites are subhedral to euhedral, randomly distributed, and some are fractured. They mainly occur embedded within pigeonite grains or between augite and titanomagnetite crystals. The cumulus apatite grain selected for FIB/TEM studies is closely intergrown with titanomagnetite and Carich pyroxene and the FIB foil was cut perpendicular to the elongation direction of the crystal (Fig. 1b in Martínez et al., 2023a). The region contains five other apatite grains, ranging from ~10 to ~60 μm in size (Fig. 2c in Martínez et al. 2023b). TEM work reveals that the apatite grain sampled by the FIB section is a single crystal, except for a small (2 μm-sized square region), compositionally distinct polycrystalline region (dashed rectangle in Fig. 2a in Martínez et al.,

2023b). The apatite contains a \sim 3 µm-sized melt inclusion, which is described in Martínez et al. (2023b), and a fragmented vein, 100-200 nm wide, crosscutting the apatite FIB section (Fig. 5b in Martínez et al., 2023a).

The studied apatite grain has a composition consistent with other apatites in NWA 998 reported in the literature (e.g., Treiman and Irving, 2008; McCubbin et al., 2013) (Fig. 2), with an average Cl/F (wt%) ratio of 2.11 (Table 1). The missing component is likely dominated by vacancies (Martínez et al., 2023a), given that Channon (2013) only measured 0.07-0.11 wt% H₂O in NWA 998 apatite using secondary ion mass spectrometry, yet NWA 998 apatites have the highest missing component abundances of all nakhlites, commonly higher than 30 mol% (Fig. 2).

Mineralogy and morphology of the vein in NWA 998 apatite

The studied FIB section contains some fractures that are fragmented and curved (Figure 5b in Martínez et al. 2023a), very different from the straight and parallel fractures found in another FIB section from a different apatite grain extracted in the same meteorite (see Fig. 5a in Martínez et al., 2023a). However, the two FIB sections are at different crystallographic orientations with respect to one another (90°), which probably accounts for the difference in the characteristics of the fractures. Based on electron diffraction patterns, the fractures are parallel to (100), one of the known cleavage planes, albeit imperfect, in apatite. Bright-field TEM images show that the fractures are partially filled with a nanocrystalline phase (~200 nm wide) that diffraction patterns show consists of apatite (Fig. 3a,b). Distinct zones of apatite are present on either side of the fracture (100-200 nm wide) that are characterized by strain contrast compared to the host apatite (Fig. 3a,b). The strained apatite is in crystallographic continuity with the adjacent Cl-rich fluorapatite host with parallel [011] zone axes (Fig. 3a,b). These fractures were completely filled veins before sample preparation, but holes probably developed preferentially

during FIB sample preparation. Bright-field TEM and dark-field STEM images show that the interface between the host apatite and the nanocrystalline apatite in the vein is sharp (Fig. 3). In addition, dark-field STEM images reveal that the vein contains nano-porosity (Fig. 3c,d), which shows some complexity. Nano-pores differ from holes in that they are smaller (~1 nm) and preserve a bimodal texture and distribution within the filled parts of the vein, whereas holes resulting from the FIB thinning process are larger (100 nm-wide) and smooth. Nano-pores are rounded and occur in a trail at the outermost edges of the vein, close to the interface with the host apatite, but are larger (~3-5 nm), more elliptical to tubular, and less abundant in the center of the vein (Fig. 3c,d).

Qualitative STEM-EDS analyses indicate that apatite in the vein consists of fluorapatite (~3 wt% F and ~1 wt% CI) and a SiO₂-rich phase (10.4 wt% SiO₂, Table 1), although the vein shows variability in composition. Details of the compositional changes in the apatite across the vein-host interface (yellow dashed lines in Fig. 4a) were obtained by STEM-EDS X-ray intensity line profiles measured on the JEOL 2010F. In Figure 4, we have plotted different X-ray intensity ratios to illustrate this trend more clearly as the line profile shows significant noise. It is important to note that the X-ray intensity decreases into the vein due to preferential ion thinning, so the absolute X-ray intensity does not give an accurate representation of the elemental behavior across the vein. Therefore, additional quantitative line profiles were measured using the JEOL NEOARM to better illustrate element variations (Ca, O, F, Cl, Si, and P, atom%) across different parts of the vein (Fig. 5). The F/Cl ratio within the vein is variable with an overall increase of F over Cl with respect to the host Cl-rich fluorapatite (Fig. 4), but Figure 5 shows that the increase in F concentration occurs exclusively at the vein edges, indicating the presence of F-rich apatite (green line in Fig. 5). However, the increase in F at the edges of the vein is not developed

homogeneously and is absent in some line profiles. In some cases, the increase in F is coincident with a convergence in the Ca and P concentrations (e.g., Fig. 5b). Compositional variations might also be attributed to effects due to a complex low angle interface between the apatite vein filling. The Si/P and Ca/P ratios also increase significantly in the vein. Based on the substitution PO₄³⁻ + O²⁻ = SiO₄⁴⁻ + OH⁻, we infer that silica is not bonded in the apatite structure, because the Ca/P ratio does not increase with increasing Si content (Fig. 4b). Instead, we attribute the elevated Si concentrations to the presence of a silica-rich phase that is located at the center of the vein. This behavior is best illustrated in Figure 5d, where the Si peak is accompanied by a decrease in Ca and P concentrations. Besides, some line profiles show that the Si-rich phase might also be enriched in P and depleted in Ca. Finally, the line profile in Figure 4 also reveals a slight increase in Si concentration at one end of the X-ray intensity profile that is not accompanied by an increase of the Ca/P ratio, which could suggest that the host apatite could contain nano-inclusions of a different phase.

High-resolution TEM imaging of apatite in the vein shows that lattice planes are continuous and straight, with no evidence of domains, such as those observed in the host apatite by Martínez et al. (2023a). However, the nanostructure exhibits complex contrast differences (Fig. 6a). Randomly distributed, irregular regions of amorphous material intermixed with crystalline apatite are also apparent in HR-TEM images, likely the source of silica in the vein (Table 1, Fig. 6b), and the reason that Ca and P concentrations in the line profiles are not consistent with apatite within the vein (Fig. 5). Based on the appearance of the vein, the crystallographic continuity between host and vein apatites, the changes in composition, the presence of nano-porosity, and the occurrence of nanometer regions of amorphous material in the

vein, we suggest that fluorapatite on the vein edges is an epitaxial overgrowth caused by a fluid-mediated process (dissolution-reprecipitation).

Discussion

232

233

234

235

236

237

238

239

240

241

242

243

244

245

246

247

248

249

250

251

252

253

254

255

Previous studies have focused on using apatite to gain insights into the volatile history and budget in the martian mantle and crust (e.g., Howarth et al., 2015; McCubbin and Nekvasil, 2008; McCubbin et al., 2013; Birski et al., 2019; Brounce et al., 2022). However, none of these studies have used apatite to constrain the conditions of the later, shallower, aqueous brine that altered the nakhlite parental rocks forming secondary, low-temperature minerals. This is simply because apatite is a primary mineral that crystallized at the final stages of the nakhlite parental melt during cooling and is not a late, secondary product. However, in this study we demonstrate that NWA 998 apatite can show evidence of fluid-mediated signatures when examined at the micron-scale by TEM. In the discussion that follows, we infer the characteristics of the metasomatic replacement that formed the fracture-filling vein in a cumulus apatite grain in NWA 998, we estimate the temperature of the altering fluid, discuss possible formation processes of the vein (terrestrial versus martian alteration), and place our observations within the context of the major late-stage hydrothermal system reported in the nakhlites. Finally, we discuss the implications of our findings for larger scale processes. The fragmented vein in NWA 998 apatite consists of fluorapatite and a SiO₂-rich phase that crosscuts a single crystal F-bearing chlorapatite grain with subgrain microstructures. The discovery of the vein represents a subsolidus process that only appears to have affected apatite at extremely localized scales.

Metasomatic replacement along cleavage planes of NWA 998 apatite

The vein has the following characteristics: it is multiphase (fluorapatite is present at the vein margins and a Si-rich phase is present within the core of the vein), exhibits porosity, contains nanometer regions of amorphous material, and has a sharp boundary interface between

the vein and the parent F-bearing chlorapatite (Figs. 3-5). All these characteristics are indicative of a coupled dissolution-reprecipitation process caused by a fluid (Yanagisawa et al., 1999; Putnis and Putnis, 2007; Engvik et al., 2009). Although replacement reactions have been observed to occur mostly along grain boundaries, they have also been observed inside crystals (e.g., Engvik et al., 2009). Chlorine is not completely absent in the vein apatite (0.8-1.1 wt% Cl, compared to 3.1 in host apatite), but previous experiments have demonstrated that a small amount of Cl can remain in the crystals after ion exchange under hydrothermal conditions (Yanagisawa et al., 1999).

Therefore, the vein records the presence of fluids after crystallization of NWA 998 apatite and serves as an example of fluid-mediated apatite replacement that generates apatite of different composition. The composition of new apatite that precipitates from the fluid is thermodynamically more stable (Pollok et al., 2011; Raufaste et al., 2011) and is mainly governed by the characteristics of the fluid phase from which it is precipitating, such as the composition of the fluid, the pH, the fluid to mineral (F/M) ratio, and the temperature and pressure (Kusebauch et al., 2015). In a ternary plot of apatite X-site occupancy (mol%), the composition of the vein lies in a field that is significantly distinct from the composition of the host apatite and other apatites in NWA 998 (Fig. 2).

Previous experiments that focused on ion exchange of Cl⁻ by OH⁻ and by F⁻ have shown that in general, higher concentrations of the alkaline solution and higher F/M ratio, favor more extensive replacement. These experiments have demonstrated that a F-containing solution will be depleted during interaction with Cl-apatite, and that F concentration in the new apatite is strongly dependent on overall F⁻ concentration in the fluid, but not on Cl⁻ concentration (Kusebauch et al., 2015), because F is highly compatible and strongly partitions into apatite compared to Cl (Zhu

and Sverjensky, 1991). Therefore, a fluid that circulates through Cl-rich apatite will end up Cl-enriched and F-depleted through the reaction:

 $Cl-F-OH-Ap + Cl(?)-(F)-OH^-(aq) \rightarrow F-OH(?)-Ap + Cl^-(aq)$

279

280

281

282

283

284

285

286

287

288

289

290

291

292

293

294

295

296

297

298

299

300

301

We propose that a fluid initially out of equilibrium with the apatite infiltrated through the cleavage pathways and promoted dissolution of the parent F-bearing chlorapatite. The discovery of amorphous material (10 nm-scale) intermixed with crystalline fluorapatite (Fig. 6b) provides evidence for dissolution and low temperature reprecipitation. Consequently, chemical components were redistributed (ion exchange) between both the parent apatite and the fluid. New apatite grew first epitaxially on the walls of the vein, from the surfaces of the crystals that were in contact with the reaction media (Yanagisawa et al., 1999), and in local equilibrium with the fluid from which it was crystallizing (e.g., Kusebauch et al., 2015). The change in composition indicates that the fluid evolved towards Cl-enriched and F-, OH-depleted (lower OH⁻ activities), and indicates that the fluid was a very limited reservoir. Since water dissociates to H⁺ and OH⁻, for a NaCl-bearing fluid, as OH is incorporated into the apatite structure, HCl forms and the pH drops. Therefore, the amorphous silica that formed last (center of the vein) formed in equilibrium with a fluid that was already depleted, because F and OH were already consumed (Kusebauch et al., 2015) (Fig. 6c-e). However, we cannot rule out the possibility that the amorphous silica is hydrated and incorporated OH as well. The fact that new fluorapatite only crystallized at the margins of the vein indicates that the amount of dissolution of parent apatite was extremely low, and that the limited fluid reservoir was effectively acting like a closed system.

The presence of nanometer-scale porosity observed in the vein (Fig. 3c,d) provides further evidence of a replacement reaction in apatite and is consistent with dissolution under hydrothermal conditions. Two kinds of porosity occur in the vein: smaller and more abundant

pores at the edges of the vein and larger and less abundant at the center (Fig. 3c). It is plausible that the smaller pores might be nanometer tunnels in three dimensions, parallel to the c axis of apatite (e.g., Young, 1980; Brenan, 1993; Yanagisawa et al., 1999). First, the introduction of an aqueous brine that was out of equilibrium with apatite triggered the dissolution of F-bearing chlorapatite, where Ca and P dissolved into the fluid at a very localized scale and changed its composition. The smaller pores at the vein interface are evidence of dissolution of parent apatite, produced before fluorapatite began to crystallize. Pores were cavities filled with fluid that formed a continuous network that allowed fast exchange of ions between the host apatite and the fluid (e.g., Engvik et al., 2009). Calcium, P, and F went into solution and were then used to form new fluorapatite, whereas Cl was transported away in the fluid phase. We cannot establish whether the new apatite on the edges of the vein incorporated more OH during apatite growth. The presence of amorphous silica in the vein suggests that some mass loss on the local scale must have occurred in order to allow growth of the new phase. The larger porosity at the center of the vein formed last, being the last fluid-filled pore spaces that were left over from the crystallization of the Si-rich phase, because of the mass loss produced by dissolution of host Fbearing chlorapatite.

302

303

304

305

306

307

308

309

310

311

312

313

314

315

316

317

318

319

320

321

322

323

324

An important question is whether the F taken up into the apatite was derived from dissolution of the primary apatite or if additional F was derived from the fluid. An experimental study by Kusebauch et al. (2015) provides some insight into how F might have behaved. Kusebauch et al. (2015) reacted synthetic endmember chlorapatite with various solutions containing NaCl, KOH, and NaF at temperatures ranging from 400 to 700 °C to investigate the replacement products and understand the behavior of halogens during metamorphism. Epitaxial apatite is observed in all of the products to different degrees. Apatite reacting with the NaF

solution was the only experiment that produced fluorapatite with the three-endmember solid solution, hence F was completely derived from the external fluid. Experiments demonstrated that temperature has a major effect on the composition of epitaxial apatite, X_{OH} increasing with temperature (Zhu and Sverjensky, 1991; Yanagisawa et al., 1999). Replacement with intermediate and low concentration NaF solutions produced F-rich apatite with variable compositions, whereas replacement with highly concentrated (1.5–3 wt%) NaF solutions lead to the formation of almost pure fluorapatite with a temperature dependent portion of the Cl component as follows: at 400 and 500°C, X_{Cl} was 0.5 and at 600-700°C, the product was almost pure fluorapatite and only traces of Cl were measured. Based on these data, we infer that the epitaxial vein in NWA 998 apatite formed at less than 400°C (see Fig. 8 in Kusebauch et al., 2015) and the solution that infiltrated into the opened cleavage planes likely contained some F. The observed low porosity in the vein (Fig. 3) also indicates that little material was dissolved, and that the reaction was roughly isovolumetric. Therefore, to account for the increase in the F/Cl ratio observed in the vein (there are $\geq 2x$ more F in the vein compared to the host apatite, Table 1, Figs. 4-6) and in order to maintain the same volume, we argue that some Cl and F from the host apatite was also dissolved into solution and thus, some of the F in the new apatite was derived from the precursor F-rich chlorapatite. Another possibility would be that there was simply anionic exchange between the existing F-rich chlorapatite and the F-bearing solution and hence, no dissolution occurred, but this is inconsistent with the amorphous regions observed with HR-TEM (Fig. 6a,b). Therefore, an important implication that needs to be considered is whether late hydrothermal fluids interacting with the nakhlites could result in Cl-enriched fluids. Based on our example, the injection of fluid into the crystal occurred on a very short timescale and the fluid 'quenched' inside the crystal, acting as a closed system. However, future work on other

325

326

327

328

329

330

331

332

333

334

335

336

337

338

339

340

341

342

343

344

345

346

grains could potentially reveal larger-scale veins showing that the fluid could have circulated and travelled further distances.

Although OH is more readily incorporated into replaced or epitaxial apatite at higher temperature (Yanagisawa et al., 1999; Kusebauch et al., 2015), the change in composition of apatite on the edges of the vein indicates that there could have been a dependency on the amount of OH in the solution despite the low temperature. For experiments using NaCl, as the fluid becomes more acidic, OH⁻ enters the apatite structure. Therefore, in the Kusebauch et al. (2015) experiments, the constant change of pH (as HCl is produced during replacement) also affected the composition of replaced apatite. On the contrary, experiments using KOH are buffered and OH activity is fixed, resulting in a constant composition of replaced apatite (Kusebauch et al., 2015).

Sequence of events that formed the vein

A potential sequence of events to explain the formation of the veins is illustrated in Figure 7. Cleavage planes of apatite were fractured and opened either by an impact or simply by settling in the magma chamber. Alternatively, infiltration of fluids along planes of weakness, such as cleavage planes, caused veins to open and widen (e.g., Lee et al., 2015a), but the fluid was not necessarily circulating. The fractionation between F and Cl in the epitaxial apatite overgrowing the host along the edge of the vein requires a closed system within the vein and not a continuous reservoir of fluid, because that would have constantly changed the Cl concentration in the fluid (i.e., lower concentration of Cl in the fluid). It is plausible that the veins formed very quickly (e.g., hydrothermal fluid 'quenched' into the cooler host apatite) and acted as a closed system (e.g., fluid injected during an impact), with insufficient time for interaction between the larger fluid reservoir in the host rock.

Temperature of formation of the vein

The duration of the Kusebauch et al. (2015) experiments was between 7 to 17 days and experiments were terminated by quenching at cooling rates of 100°C/min, because the study was focused on long-duration fluid mineral interactions. This suggests that the veins in NWA 998 apatite could have formed in only a few days to a few weeks. The fact that the vein in NWA 998 apatite preserves a compositional difference and a sharp interface with the host apatite (Fig. 3) indicate that they formed at low temperatures (lower than 400 °C) and/or cooled very quickly in order to prevent diffusional equilibration and eradication of the microstructures (i.e., coarsening of the porosity), especially taking into account that the veins are extremely thin, less than a micron in width. To better estimate the temperature of formation of the veins, we have used the equation from Li et al. (2020) to calculate diffusion coefficients (D*) of Cl in apatite as a function of temperature (equation 1). The equation was obtained from experiments performed on natural Durango apatite between 800 and 1100 °C, 1 atm, and oxygen fugacity at the wüstite-magnetite buffer, using a multicomponent diffusion model.

$$D_{Cl}^* = 7\binom{+12}{-4} \times 10^{-5} \times \left[exp^{\left(\frac{-294(\pm 12)KJ/mol}{RT}\right)} \right] m^2/s \tag{1}$$

Diffusion coefficients calculated using equation (1) from Li et al. (2020) have been extrapolated to temperatures below 800 °C. Applying a diffusion distance of Cl in the vein of 100 nm (Figs. 3,4), we have calculated different times of Cl diffusion as a function of temperature using Fick's second law of diffusion (equation 2):

390
$$t = \frac{1}{2 \times D_{Cl}^*} x^2 \tag{2}$$

Where x is the diffusion distance and t is time.

The results are shown in Figure 8. In order to extract the temperature of formation of the veins in NWA 998 from Figure 8, we have considered that the veins formed at the same time as

other secondary minerals in the nakhlites. Some studies have used noble gases to date the formation of the secondary alteration phase 'iddingsite' in the nakhlites and obtained an age of ~650 Ma (Swindle et al., 2000, in the Lafayette meteorite). However, determining the age(s) of formation of secondary minerals in the nakhlites is challenging, because the minerals are fine-grained, difficult to separate from the host, and it is possible that Martian atmospheric gases (e.g., ⁴⁰Ar) were implanted after the formation of the phyllosilicates occurred (e.g., during shock).

However, if the vein in NWA 998 has a similar age as Lafayette 'iddingsite' veins, formed during a shock event that triggered a hydrothermal system in the nakhlites (e.g., Changela and Bridges, 2010) (discussed below), we infer that the vein quenched at about 300 °C (blue star in Fig. 8). A temperature of formation higher than 300 °C is unlikely, because the compositional difference would have been eradicated very quickly and/or would not had been preserved for an extended geologic time period. Nonetheless, this temperature must be taken as an estimate, because it is possible that the diffusion coefficients for Cl obtained from Li et al. (2020) at high temperatures (equation 1) cannot be extrapolated to lower temperatures reliably, because the diffusion mechanism may not be the same over such a wide temperature interval.

Processes that could have formed the vein

Terrestrial alteration

Northwest Africa 998 is a find with a terrestrial residence age of $6,000 \pm 1,000$ years (Nishiizumi et al., 2004). Although this is a relatively short period of time on geologic timescales, a terrestrial origin for the formation of the epitaxial fluorapatite veins needs to be considered, because liquid water and water-soluble salts in hot deserts have been shown to cause weathering of meteorites (e.g., Barrat et al., 1998; Lee and Bland, 2004; Al-Kathiri et al., 2005;

Bland et al., 2006). Zurfluh et al. (2013) examined a set of ordinary chondrites found in the desert of Oman and found that the most common secondary minerals after hydroxides and iron oxides are gypsum and calcite, and that bromine and fluorine are normally below detection limits. Indeed, calcite and barite in nakhlite finds have been interpreted to be terrestrial in origin (Coulson et al., 2007; Tomkinson et al., 2015; Hallis et al., 2017).

In NWA 998, calcite veins and Ca-sulfates have been reported as mineral products of desert weathering (Treiman and Irving, 2008; Hicks et al., 2014), but detailed studies of terrestrial alteration products in NWA 998 are limited, and analyses of hydrous silicate phases in this meteorite are lacking. However, Cartwright et al. (2013) used ⁴⁰Ar-³⁹Ar ages and noble gas (Cl, Br, I) abundances to determine hydrous fluids and terrestrial weathering products in NWA 998. The study found isotopic evidence of a Cl-rich fluid that matches the martian atmosphere and argued that it might be hosted in fluid inclusions. Additionally, the authors determined the presence of another fluid with elevated I/Cl ratios, but were unable to discriminate between *in situ* low temperature terrestrial contamination or martian alteration.

The studied thin section of NWA 998 does not show apparent signs of terrestrial alteration. No crosscutting calcite veins or phyllosilicates have been observed either by BSE-SEM or TEM imaging. Transmission electron microscopy observations of the apatite grain examined in this study shows that it is a single crystal that preserves a melt inclusion (Martínez et al., 2023b). The melt inclusion exhibits minimal syn- and post-entrapment effects and largely remained as a closed system (Martínez et al., 2023b). Notably, pore space around the edge of the inclusion lacks any evidence of carbonates, sulfates, or phyllosilicates.

Based on our observations, several lines of evidence can be proposed that argue against a terrestrial origin for the F-rich epitaxial apatite vein, including: (i) the small scale of the vein and

the preservation of the compositional difference indicates that vein formation occurred very rapidly as a result of injection of a fluid into cold rock rather than extended hydrothermal circulation through the cumulus nakhlite pile (Figs. 3-6); (ii) weathering of apatite observed in meteorites from the Oman desert reported by Zurfluh et al. (2013) results in the formation of Febearing phosphate, not F-bearing apatite; (iii) the composition of the fluid (F- and possibly OHrich and Cl-poor) that formed the vein is not expected for a terrestrial weathering fluid (i.e., rainwater or soil-pore water derived from rainwater by dissolution of salts). Zurfluh et al. (2013) found that hot desert soils have significant, albeit variable concentrations of chloride, which is readily transported into meteorites during weathering, resulting in some Cl-rich weathering products, such as bischofite (MgCl₂*6H₂O). Although the meteorites studied by Zurfluh et al. (2013) are ordinary chondrites, not martian meteorites, the principle that the solutions would be Cl-rich still applies. Therefore, even if geochemical conditions during hot desert weathering favored the formation of apatite, it would be expected to be Cl-rich rather than the reverse, as is observed in NWA 998; (iv) the precipitation of calcite in NWA 998 reported in the literature requires alkaline conditions, whereas apatite dissolves at more acidic conditions (e.g., Valsami-Jones et al., 1998). Our proposed mechanism of vein formation involving dissolution and reprecipitation of apatite requires a fluid geochemistry that is not compatible with the conditions required for precipitation of calcite; (v) the calculated temperature of formation of the vein (300 °C) is too high for hot desert altering fluids, and finally; (vi) the lack of any other potential terrestrial alteration products in any of the FIB sections examined in NWA 998 also supports a pre-terrestrial origin for the epitaxial apatite veins in NWA 998.

Hydrothermal system triggered by a shock event

440

441

442

443

444

445

446

447

448

449

450

451

452

453

454

455

456

457

458

459

460

Several studies have confirmed that the nakhlites were subjected to shock, although it was relatively mild compared to other groups of martian meteorites (e.g., Malavergne et al., 2001; Fritz et al., 2005). One of the hypotheses that has gained popularity is that an impactinduced hydrothermal system adjacent to the nakhlite parent rocks fractured the nakhlites and formed secondary alteration minerals (Changela and Bridges, 2010). Whether the veins observed in NWA 998 apatite occurred during this impact event or the two events occurred independently (first, the impact and later, a fluid percolated through the fractures) is not clear from this study, but the following observations can be made: (i) there is no evidence of microscale veining in BSE imaging, thus the amount of fluid in this specific event was relatively limited or localized in scale; (ii) the small scale of the vein and the presence of compositionally distinct epitaxial apatite on the edge of the vein indicate that the vein could not have formed when the rock was at relatively high temperature and/or undergoing slow cooling, otherwise the compositional change would have equilibrated due to volume diffusion; and (iii) limited fracturing in apatite and the relatively low dislocation density and subgrain structure indicate that these features could have been caused by a process other than shock, such as crystal settling in the magma chamber or post solidification movement within the magma chamber, given the cumulus nature of the studied apatite grain. Alternatively, the vein could have formed by rapid injection of a hotter (>300 °C) hydrothermal fluid into a cold rock, where the surrounding rock 'quenched' the fluid, resulting in rapid growth of the vein apatite as fractionation between the fluid and apatite occurred. The last case would have operated at a certain distance from the nakhlite ejection site, given the lack of evidence of a high temperature event in NWA 998 or any other nakhlite, and might be compatible with an impact origin of the vein, or at the margins of the crater (see iii), as

462

463

464

465

466

467

468

469

470

471

472

473

474

475

476

477

478

479

480

481

482

postulated by Changela and Bridges (2010), but we cannot differentiate between primary subsolidus cooling and a mild impact.

Comparison with the late-stage hydrothermal system in other nakhlites

Hydrogen isotopic compositions of water found in iddingsite veins in several nakhlites show that the aqueous fluids responsible for alteration have an elevated deuterium/hydrogen (D/H) ratio compared to Earth. Hence, the aqueous fluid either equilibrated with the martian atmosphere (enriched in deuterium) or was derived directly from the hydrated martian crust (Usui et al., 2015). The only meteorites with 'iddingsite' veins that have been dated are Lafayette and Y-000593, giving an age of 633 ± 23 Ma (Swindle et al., 2000; Borg and Drake, 2005). The data thus show that liquid water that altered these two meteorites could not be derived from the same magmatic episode that formed the nakhlites. This is consistent with the fluid that affected NWA 998 (F-,Si-rich, Cl-poor), because magmatic fluids contain 1.36 wt% Cl (McCubbin et al., 2013).

In NWA 817, some authors have argued that the water responsible for alteration was derived from the martian mantle, because 'iddingsite' in NWA 817 has unusually low δD ([(D/H)_{sample}/(D/H)_{V-SMOW} - 1] \times 1000) values (Gillet et al., 2002; Meunier et al., 2012). This observation suggests that NWA 817 could have sampled a different aqueous fluid derived from the same magmatic system that formed the nakhlite lavas. However, Lee et al. (2018) attributed the low δD value to terrestrial contamination, as the hydrogen isotopic system is particularly susceptible to re-equilibration (Hallis et al., 2012). Furthermore, Lee et al. (2018) argued that the presence of terrestrial calcite along olivine vein walls supports a terrestrial contribution and the lack of Cl within NWA 817 'iddingsite' indicates the fluid was not magmatic. They concluded that the alteration formed under the same physico-chemical conditions and belongs to the same

liquid water reservoir as other nakhlites. In this case, the fluid was derived from the martian crust or atmosphere, and the authors favor volcanic activity for the heat source rather than a nearby impact (Lee et al., 2018).

507

508

509

510

511

512

513

514

515

516

517

518

519

520

521

522

523

524

525

526

527

528

529

The late-stage hydrothermal event represented by the epitaxial fluorapatite vein found in NWA 998 host apatite could be the same hydrothermal system that affected other nakhlites to a greater extent (e.g., Gooding et al., 1991; Treiman et al., 1993; Bridges and Grady, 1999, 2000; Gillet et al., 2002; Changela and Bridges, 2010; Cartwright et al., 2013). However, the fact that the nakhlites likely represent different magmatic pulses from the same magma source that were emplaced at different times, spanning crystallization ages of 94 ± 12 Ma (Cohen et al., 2017), raises the possibility of having different episodes of altering fluids (e.g., a hydrothermal system triggered by a different, mild impact event before more evolved nakhlites were emplaced). The composition of the fluid (Cl-poor, F-,Si-rich) and/or the altering conditions in NWA 998 were also different from the fluid that produced 'iddingsite' veins within olivine in the other nakhlites, i.e., the presence of smectite is indicative of a moderate to alkaline pH (Mustard et al., 2008), whereas the dissolution and re-precipitation of apatite requires acidic conditions. Therefore, if the hydrothermal system represented by NWA 998 veins is the same as the major event that affected other nakhlites, the differences in fluid composition could be ascribed to having a less evolved fluid in NWA 998 (i.e., the fluid did not acquire solutes by dissolution of mesostasis glass). Furthermore, the fact that the fluid that formed the epitaxial veins in NWA 998 was very limited could be ascribed to the rock being more distal to the heat source compared to the other nakhlites. Alternatively, the epitaxial apatite veins in NWA 998 could be derived from a different fluid not sampled in other nakhlites.

Implications for the utilization of apatite to reconstruct volatile histories on Mars

Although apatite in the nakhlites is a primary mineral that crystallized close to the end of the paragenetic sequence of the parental magma, this work demonstrates that caution must be exercised when using apatite to reconstruct the volatile behavior in the martian mantle (and crust), because the magmatic F and/or Cl contents can be over- or under-estimated due to the presence of these secondary nano-scale veins that are only observed by FIB/TEM studies. Future work on other apatite grains will help quantify the occurrence of these veins to better interpret the volatile history and budget on Mars.

Conclusions

The nakhlites are martian meteorites formed from basaltic magmas that were emplaced at different depths in the martian crust forming cumulate rocks. A later, hydrothermal event interacted with the nakhlite cumulates and produced secondary mineral assemblages, such as smectite clays and Fe-rich carbonates.

We report epitaxial fluorapatite occurring at the margins of a vein (100-200 µm in width) and a silica-rich phase occurring at the core of the vein, filling opened cleavage planes in NWA 998 cumulus F-bearing chlorapatite. The veins record a fluid-mediated replacement reaction of chlorapatite that generated more stable fluorapatite in a closed system plus a residual silica-rich phase. Parent F-bearing chlorapatite was dissolved, new fluorapatite crystallized in local equilibrium with the fluid, and the fluid became Cl-enriched. The fluid was slightly acidic, and the estimated temperature of the hydrothermal system is 300 °C, based on Cl diffusivities by Li et al. (2020) and the width of the vein. Fluid infiltration occurred after primary magmatic crystallization and could have been triggered by a mild impact.

Several lines of evidence, such as the fluid composition, kinetics, and temperature, indicate that the epitaxial fluorapatite veins are pre-terrestrial and represent a late-stage alteration event in

the crust of Mars, ruling out magmatic fluid activity. The epitaxial veins in NWA 998 could have formed from the same hydrothermal system that affected other nakhlites or represent a sample of a different aqueous fluid, because the nakhlites were emplaced into the martian crust over extended periods of time.

This is the first study that demonstrates the presence of nanometer-scale veins in apatite and has significant implications for the large-scale hydrothermal system that affected the nakhlites. The present study also provides an important context for understanding the chemical and isotopic compositions of apatite, notably the potential for modification of the primary compositions by late-stage fluid interactions.

Acknowledgments

We would like to thank the Institute of Meteoritics for access to the thin sections of the two nakhlites used in this study. Electron microscopy was carried out in the Electron Microbeam Analysis Facility, Department of Earth and Planetary Sciences, University of New Mexico, a facility funded by NSF, NASA and the state of New Mexico. The acquisition of the JEOL NEOARM AC-STEM at the University of New Mexico was supported by NSF grant DMR-1828731. The Wilberforce apatite standard was provided by Zachary Sharp. This work was supported and funded by NASA Cosmochemistry Grant NNX15AD28G and NASA Emerging Worlds Grant 80NSSC18K0731 to A. J. Brearley.

References

- Al-Kathiri A., Hofmann B. A., Jull A. J. T., and Gnos E. 2005. Weathering of meteorites from Oman: Correlation of chemical and mineralogical weathering proxies with 14C terrestrial ages and the influence of soil chemistry. *Meteoritics & Planetary Science* 40:1215–1239.
- Barrat J. A., Gillet P., Lecuyer C., Sheppard S. M. F., and Lesourd M. 1998. Formation of carbonates in the Tatahouine meteorite. *Science* 280:412–414.
- Beck, P., Barrat, J. A., Gillet, P., Wadhwa, M., Franchi, I. A., Greenwood, R. C., Bohn, M.,
 Cotten, J., van de Moortèle, B. and Reynard, B. 2006. Petrography and geochemistry of

- the chassignite Northwest Africa 2737 (NWA 2737). *Geochimica et Cosmochimica Acta* 70:2127–2139.
- Birski, Ł., Słaby, E., Chatzitheodoridis, E., Wirth, R., Majzner, K., Kozub-Budzyń, G. A., Sláma
- J., Liszewska K., Kocjan I., and Zagórska, A. 2019. Apatite from NWA 10153 and NWA
- 583 10645—The key to deciphering magmatic and fluid evolution history in nakhlites.
- 584 *Minerals* 9:695.
- Bland P. A., Zolensky M. E., Benedix G. K., and Sephton M. A. 2006. Weathering of chondritic meteorites. In Meteorites and the early solar system II, edited by Lauretta D.
- S. and McSween H. Y. Tucson, Arizona: The University of Arizona Press.
- Borg, L. and Drake, M. J. 2005. A review of meteorite evidence for the timing of magmatism and of surface or near-surface liquid water on Mars. *Journal of Geophysical Research:* Planets 110:E12.
- Brenan, J. 1993. Kinetics of fluorine, chlorine and hydroxyl exchange in fluorapatite. *Chemical Geology* 110:195–210.
- Breton, H. 2017. Petrology and geochemistry of the nakhlite meteorites: Tracking complex
 igneous and aqueous processes on Mars during the Amazonian. Doctoral dissertation,
 University of Glasgow.
- Bridges, J. C. and Grady, M. M. 1999. A halite-siderite-anhydrite-chlorapatite assemblage in
 Nakhla: Mineralogical evidence for evaporites on Mars. *Meteoritics & Planetary Science* 34:407–415.
- Bridges, J. C. and Grady, M. M. 2000. Evaporite mineral assemblages in the nakhlite (martian) meteorites. *Earth and Planetary Science Letters* 176:267–279.
- Bridges, J. C., Smith, M. P., Grady, M. M., 2000. Progressive evaporation and relict fluid inclusions in the nakhlites. 31st Proceedings of Lunar and Planetary Science Conference, abstract #1590.
- Bridges, J. C., Catling, D. C., Saxton, J. M., Swindle, T. D., Lyon, I. C., and Grady, M. M. 2001.

 Alteration assemblages in Martian meteorites: Implications for near-surface processes. *Space Science Reviews* 96:365–392.
- Brounce, M., Boyce, J. W., and McCubbin, F. M. 2022. Sulfur in apatite from the Nakhla
 meteorite record a late-stage oxidation event. *Earth and Planetary Science Letters* 595:117784.
- Cao, H., Chen, J., Fu, X., Xin, Y., Qi, X., Shi, E., and Ling, Z. 2022. Raman spectroscopic and
 geochemical studies of primary and secondary minerals in Martian meteorite Northwest
 Africa 10720. *Journal of Raman Spectroscopy* 53:420-434.

- 613 Cartwright, J. A., Gilmour, J. D., and Burgess, R. 2013. Martian fluid and Martian weathering 614 signatures identified in Nakhla, NWA 998 and MIL 03346 by halogen and noble gas
- analysis. *Geochimica et Cosmochimica Acta* 105:255–293.
- Changela, H. G. and Bridges, J. C. 2010. Alteration assemblages in the nakhlites: Variation with depth on Mars. *Meteoritics & Planetary Science* 45:1847–1867.
- Channon, M. B. 2013. Oxygen isotopes and volatiles in Martian meteorites. Doctoraldissertation, California Institute of Technology.
- 620 Cohen, B. E., Mark, D. F., Cassata, W. S., Lee, M. R., Tomkinson, T., and Smith, C. L. 2017.
- Taking the pulse of Mars via dating of a plume-fed volcano. *Nature Communications* 8:1-622 9.
- 623 Coulson, I. M., Beech, M., and Nie, W. 2007. Physical properties of Martian meteorites: Porosity and density measurements. *Meteoritics & Planetary Science* 42:2043–2054.
- Engvik, A. K., Golla-Schindler, U., Berndt, J., Austrheim, H., and Putnis, A. 2009. Intragranular replacement of chlorapatite by hydroxy-fluor-apatite during metasomatism. *Lithos* 112:236–246.
- Fritz, J., Artemieva, N., and Greshake, A. 2005. Ejection of Martian meteorites. *Meteoritics & Planetary Science* 40:1393–1411.
- Gillet, P., Barrat, J. A., Deloule, E., Wadhwa, M., Jambon, A., Sautter, V., Devouard, B.,
- Neuville, D., Benzerara, K., and Lesourd, M. 2002. Aqueous alteration in the Northwest
- Africa 817 (NWA 817) Martian meteorite. *Earth and Planetary Science Letters* 203:431–444.
- Gooding, J. L., Wentworth, S. J., and Zolensky, M. E. 1991. Aqueous alteration of the Nakhla meteorite. *Meteoritics* 26:135-143.
- Hallis, L. J. and Taylor, G. J. 2011. Comparisons of the four Miller Range nakhlites, MIL 03346,
 090030, 090032 and 090136: Textural and compositional observations of primary and
 secondary mineral assemblages. *Meteoritics & Planetary Science* 46:1787-1803.
- Hallis, L. J., and Lee, M. R. 2014. Fluid inclusions in Lafayette: a record of ancient Martian hydrology. 77th Annual Meeting of the Meteoritical Society, abstract #5134.
- Hallis L. J., Taylor G. J., Nagashima K., Huss G. R., Needham A. W., Grady M. M., and Franchi
 I. A. 2012. Hydrogen isotope analyses of alteration phases in the nakhlite Martian
 meteorites. *Geochimica et Cosmochimica Acta* 97:105–119.
- Hallis L. J., Kemppinen L., Lee M., and Taylor L. A. 2017. The origin of alteration "orangettes"
 in shergottite Dhofar 019. *Meteoritics & Planetary Science* 52:2695–2706.

- Harvey, R. P. and McSween Jr, H. Y. 1992. Petrogenesis of the nakhlite meteorites: Evidence from cumulate mineral zoning. *Geochimica et Cosmochimica Acta* 56:1655–1663.
- Hicks, L. J., Bridges, J. C., and Gurman, S. J. 2014. Ferric saponite and serpentine in the nakhlite martian meteorites. *Geochimica et Cosmochimica Acta* 136:194–210.
- Howarth, G. H., Pernet-Fisher, J. F., Bodnar, R. J., and Taylor, L. A. 2015. Evidence for the
 exsolution of Cl-rich fluids in martian magmas: Apatite petrogenesis in the enriched
 lherzolitic shergottite Northwest Africa 7755. Geochimica et Cosmochimica

653 *Acta* 166:234–248.

- Kusebauch, C., John, T., Whitehouse, M. J., Klemme, S., and Putnis, A. 2015. Distribution of halogens between fluid and apatite during fluid-mediated replacement processes. *Geochimica et Cosmochimica Acta* 170:225–246.
- Lee M. R. and Bland P. A. 2004. Mechanisms of weathering of meteorites recovered from hot and cold deserts and the formation of phyllosilicates. *Geochimica et Cosmochimica Acta* 68:893–916.
- Lee, M. R., Tomkinson, T., Hallis, L. J., and Mark, D. F. 2015a. Formation of iddingsite veins in the martian crust by centripetal replacement of olivine: Evidence from the nakhlite meteorite Lafayette. *Geochimica et Cosmochimica Acta* 154:49-65.
- Lee, M. R., MacLaren, I., Andersson, S. M. L., Kovacs, A., Tomkinson, T., Mark, D. F., and Smith, C. L. 2015b. Opal-A in the Nakhla meteorite: A tracer of ephemeral liquid water in the Amazonian crust of Mars. *Meteoritics & Planetary Science* 50:1362–1377.
- Lee, M. R., Daly, L., Cohen, B. E., Hallis, L. J., Griffin, S., Trimby, P., Boyce, A., and Mark, D.
 F. 2018. Aqueous alteration of the Martian meteorite Northwest Africa 817: Probing
 fluid–rock interaction at the nakhlite launch site. *Meteoritics & Planetary Science* 53:2395–2412.
- Li, W., Chakraborty, S., Nagashima, K., and Costa, F. 2020. Multicomponent diffusion of F, Cl and OH in apatite with application to magma ascent rates. *Earth and Planetary Science Letters* 550: 116545.
- Malavergne, V., Guyot, F., Benzerara, K., and Martinez, I. 2001. Description of new shock induced phases in the Shergotty, Zagami, Nakhla and Chassigny meteorites. *Meteoritics* & Planetary Science 36:1297–1305.
- 676 Martínez, M., Shearer, C.K., Brearley, A.J., 2023a. Nanostructural domains in martian apatites 677 that record primary subsolidus exsolution of halogens: Insights into nakhlite petrogenesis. 678 *American Mineralogist* preprint. doi.org/10.2138/am-2022-8794.
- Martínez, M., Shearer, C. K., and Brearley, A. J. 2023b. Ferro-chloro-winchite in Northwest
 Africa (NWA) 998 apatite-hosted melt inclusion: New insights into the nakhlite parent
 melt. *Geochimica et Cosmochimica Acta* 344:122–133.

- McCubbin, F. M. and Nekvasil, H. 2008. Maskelynite-hosted apatite in the Chassigny meteorite:
- Insights into late-stage magmatic volatile evolution in martian magmas. *American*
- 684 *Mineralogist* 93:676–684.
- McCubbin, F. M., Elardo, S. M., Shearer Jr, C. K., Smirnov, A., Hauri, E. H., and Draper, D. S.
- 686 2013. A petrogenetic model for the comagmatic origin of chassignites and nakhlites:
- Inferences from chlorine-rich minerals, petrology, and geochemistry. *Meteoritics &*
- 688 *Planetary Science* 48:819–853.
- Meunier A., Petit S., Ehlmann B. L., Dudoignon P., Westall F., Mas A., Albani A., and Ferrage
 E. 2012. Magmatic precipitation as a possible origin of Noachian clays on Mars. *Nature*
- *Geoscience* 5:739–743.
- Mikouchi, T., Makishima, J., Kurihara, T., Hoffmann, V. H., and Miyamoto, M. 2012. Relative
- burial depth of nakhlites revisited. 43rd Lunar and Planetary Science Conference, abstract #2363.
- Mustard, J. F., Murchie, S. L., Pelkey, S. M., Ehlmann, B. L., Milliken, R. E., Grant, J. A.,
- Bibring, J.P., Poulet, F., Bishop, J., Noe Dobrea, E., Roach, L., Seelos, F., Arvidson, R.
- E., Wiseman, S., Green, R., Hash, C., Humm, D., Malaret, E., McGovern, J. A., Seelos,
- K., Clancy, T., Clark, R., Des Marais, D., Izenberg, N., Knudson, A., Langevin,
- Y., Martin, T., McGuire, P., Morris, R., Robinson, M., Roush, T., Smith, M., Swayze,
- G., Taylor, H., Titus, T., and Wolff, M. 2008. Hydrated silicate minerals on Mars
- observed by the Mars Reconnaissance Orbiter CRISM instrument. *Nature* 454:305–309.
- Nyquist, L. E., Bogard, D. D., Shih, C. Y., Greshake, A., Stöffler, D., and Eugster, O. 2001.
- Ages and geologic histories of Martian meteorites. In *Chronology and evolution of Mars*.
- Springer, Dordrecht. Pp. 105–164.
- Pollok, K., Putnis, C. V., and Putnis, A. 2011. Mineral replacement reactions in solid solution-
- aqueous solution systems: Volume changes, reactions paths and end-points using the
- example of model salt systems. *American Journal of Science* 311:211–236.
- Putnis, A. and Putnis, C. V. 2007. The mechanism of reequilibration of solids in the presence of
- a fluid phase. *Journal of Solid State Chemistry* 180:1783–1786
- Raufaste, C., Jamtveit, B., John, T., Meakin, P., and Dysthe, D. K. 2011. The mechanism of
- porosity formation during solvent-mediated phase transformations. *Proceedings of the*
- 712 Royal Society A: Mathematical, Physical and Engineering Sciences 467:1408–1426.
- Shearer, C. K., Messenger, S., Sharp, Z. D., Burger, P. V., Nguyen, A. N., and McCubbin, F. M.
- 714 2018. Distinct chlorine isotopic reservoirs on Mars. Implications for character, extent and
- relative timing of crustal interactions with mantle-derived magmas, evolution of the
- martian atmosphere, and the building blocks of an early Mars. *Geochimica et*
- 717 *Cosmochimica Acta* 234:24–36.

- 718 Swindle, T. D. and Olson, E. K. 2004. ⁴⁰Ar-³⁹Ar studies of whole rock nakhlites: Evidence for
- 719 the timing of formation and aqueous alteration on Mars. *Meteoritics & Planetary*
- 720 *Science* 39:755–766.
- 721 Swindle, T. D., Treiman, A. H., Lindstrom, D. J., Burkland, M. K., Cohen, B. A., Grier, J. A., Li,
- B., and Olson, E. K. 2000. Noble gases in iddingsite from the Lafayette meteorite:
- Evidence for liquid water on Mars in the last few hundred million years. *Meteoritics &*
- 724 *Planetary Science* 35:107–115.
- 725 Tomkinson T., Lee M. R., Mark D. F., Dobson K. J., and Franchi I. A. 2015. The Northwest
- Africa (NWA) 5790 meteorite: A mesostasis-rich nakhlite with little or no Martian
- aqueous alteration. *Meteoritics & Planetary Science* 50:287–304.
- 728 Treiman, A. H. 2005. The nakhlite meteorites: Augite-rich igneous rocks from
- 729 Mars. *Geochemistry* 65:203–270.
- 730 Treiman, A. H. and Irving, A. J. 2008. Petrology of martian meteorite Northwest Africa 998.
- 731 *Meteoritics & Planetary Science* 43:829–854.
- 732 Treiman, A. H., Barrett, R. A., and Gooding, J. L. 1993. Preterrestrial aqueous alteration of the
- 733 Lafayette (SNC) meteorite. *Meteoritics* 28:86-97.
- Usui T., Alexander C. M. O'D., Wang J., Simon J. I., and Jones J. H. 2015. Meteoritic evidence
- for a previously unrecognized hydrogen reservoir on Mars. Earth and Planetary Science
- 736 *Letters* 410:140–151.
- Valsami-Jones, E., Ragnarsdottir, K. V., Putnis, A., Bosbach, D., Kemp, A. J., and Cressey, G.
- 738 1998. The dissolution of apatite in the presence of aqueous metal cations at pH 2–
- 7. *Chemical Geology* 151:215–233.
- 740 Wadhwa, M. and Crozaz, G. 1995. Trace and minor elements in minerals of nakhlites and
- 741 Chassigny: Clues to their petrogenesis. *Geochimica et Cosmochimica Acta* 59:3629–
- 742 3645.
- Yanagisawa, K., Rendon-Angeles, J. C., Ishizawa, N., and Oishi, S. 1999. Topotaxial
- replacement of chlorapatite by hydroxyapatite during hydrothermal ion exchange.
- 745 *American Mineralogist* 84:1861–1869.
- Young, R. A. 1980. Large effects from small structural differences in apatites. In: Proceedings of
- the International Congress of Phosphorous Compounds. Pp. 73-88.
- 748 Zhu, C. and Sverjensky, D. A. 1991. Partitioning of F-Cl-OH between minerals and
- hydrothermal fluids. *Geochimica et Cosmochimica Acta* 55:1837–1858.
- 750 Zurfluh, F. J., Hofmann, B. A., Gnos, E., and Eggenberger, U. 2013. "Sweating meteorites"—
- Water-soluble salts and temperature variation in ordinary chondrites and soil from the hot
- desert of Oman. *Meteoritics & planetary science* 48:1958–1980.

754 Figures

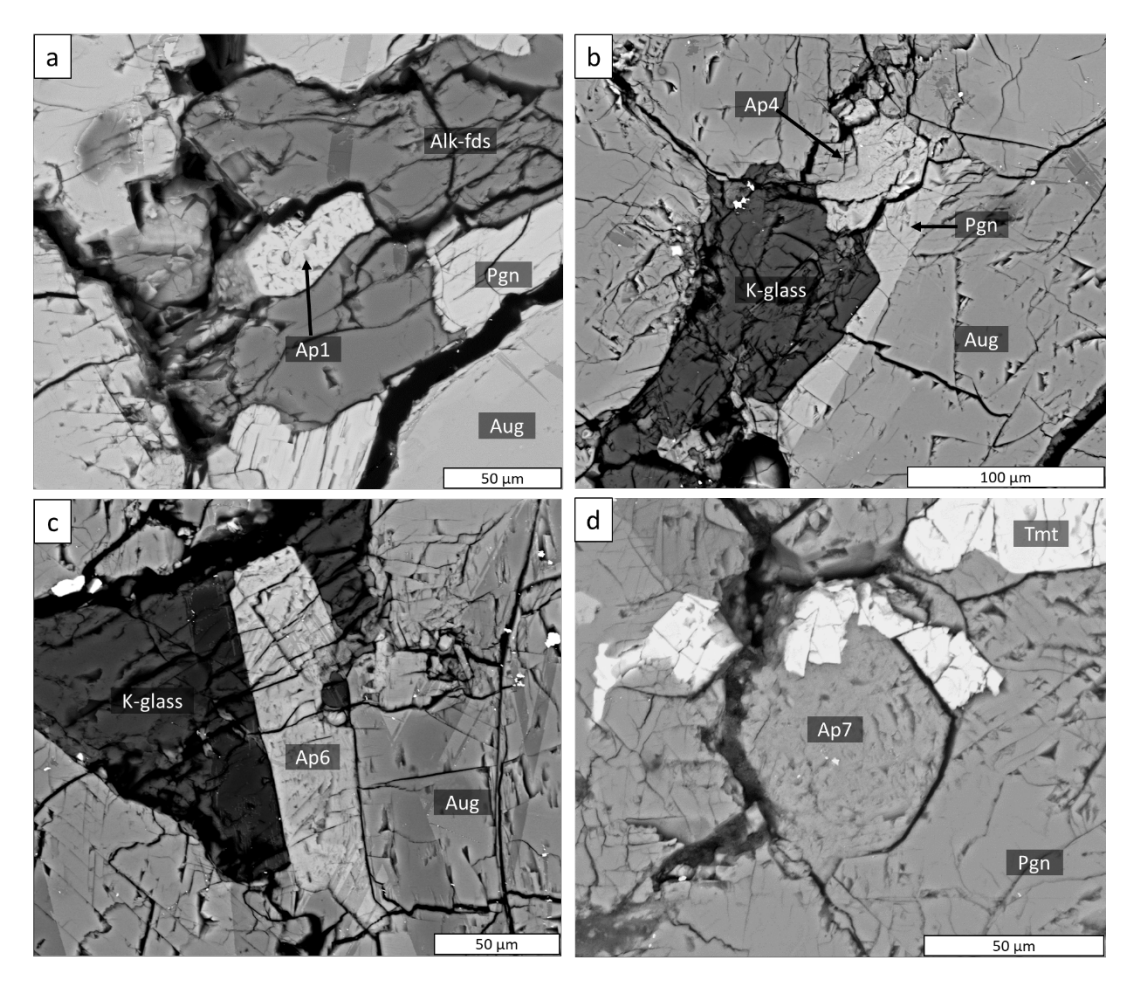


Figure 1. BSE images showing examples of cumulus apatite grains in NWA 998. Numbers referred to Figure 1 in Martínez et al. (2023a). a) Apatite 1: Anhedral cumulus chlorapatite, ~ 50 μm in size, associated with K-rich glass, pigeonite, augite, and fractures. b) Apatite 4: Anhedral cumulus chlorapatite, ~ 50 μm in size, included in zoned pyroxene and associated with K-rich glass. c) Apatite 6: Anhedral cumulus chlorapatite, ~ 120 μm long, associated with alkali-rich glass and augite. d) Apatite 7: Euhedral (basal section) cumulus apatite, 55 μm in size, intergrown with titanomagnetite and fully included in pigeonite. Legend: Ap = apatite, Tmt = titanomagnetite, Aug = augite, Pgn = pigeonite, K-glass = K-rich glass, Alk-fds = alkali-feldspar.

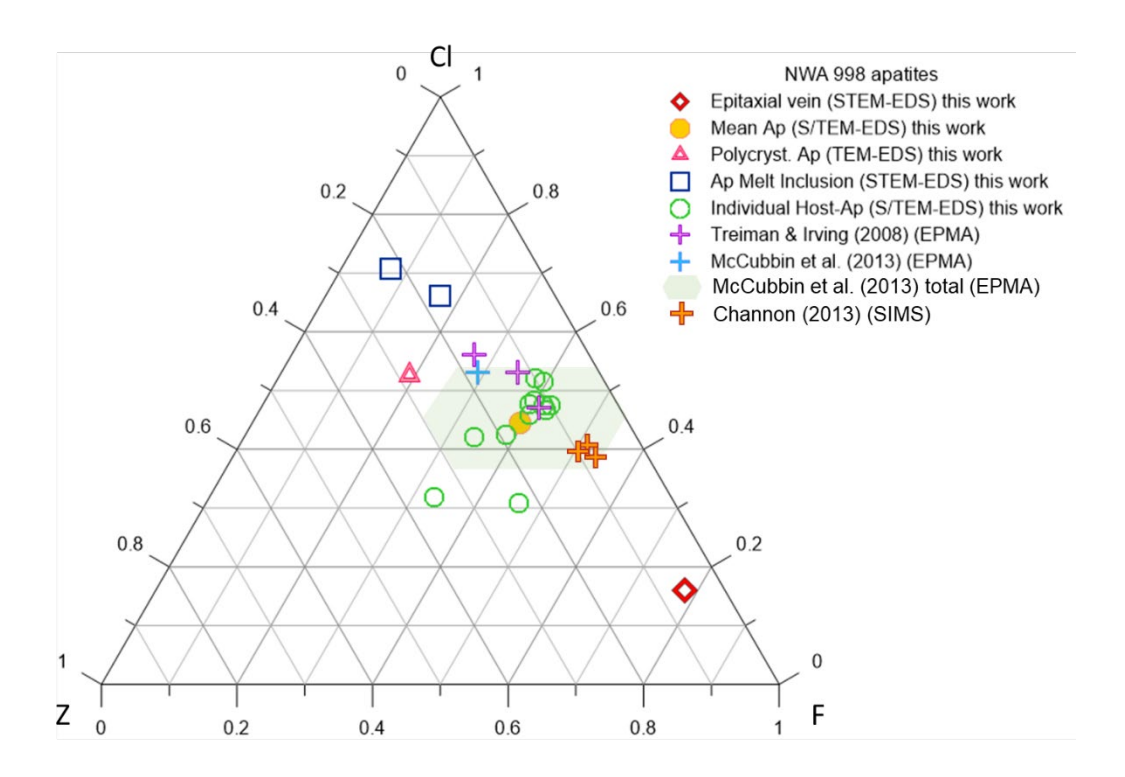


Figure 2. Ternary plot of apatite X-site occupancy (mol%) for NWA 998 apatite grains. Z = OH and/or vacancies. Fuchsia crosses represent multiple analyses of NWA 998 apatites from Treiman and Irving (2008), obtained by EPMA. The light blue cross represents mean apatite composition from McCubbin et al. (2013), obtained by EPMA, and the shadowed green area comprises the full range of values from the same study. Orange crosses represent SIMS analyses of NWA 998 apatite from Channon (2013). Individual host apatite values from this work are represented by green open circles, along with the respective averaged composition represented by a filled yellow circle. The composition of the polycrystalline apatite region is represented by pink hollow triangle, the cracked apatite associated with the melt inclusion (Martínez et al., 2023b) by hollow blue squares, and the composition of the epitaxial vein apatite, by a hollow red diamond. Modified after Martínez et al. (2023a).

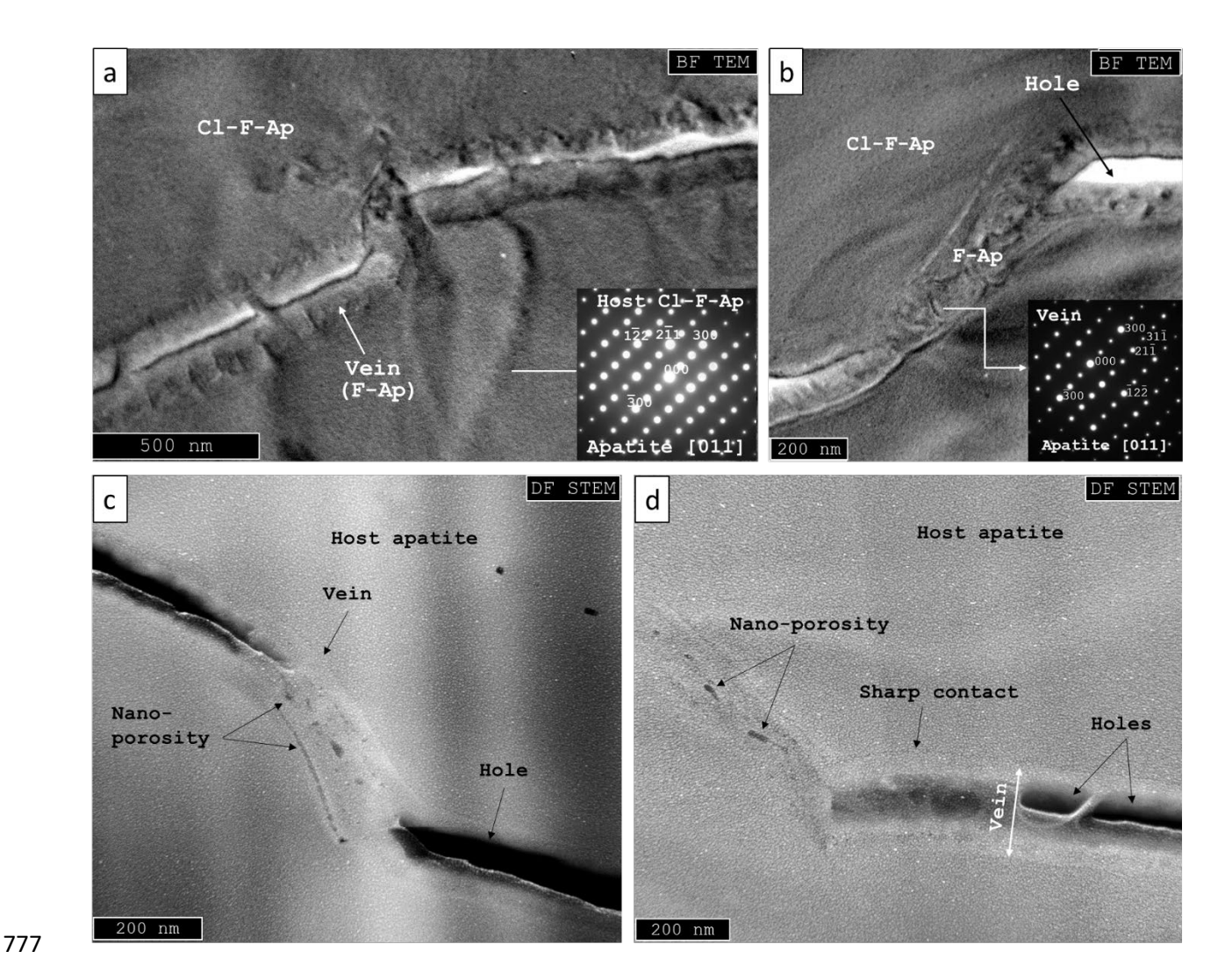


Figure 3. High-magnification S/TEM images of the thin vein, 100-200 nm in width, crosscutting the cumulus apatite grain in NWA 998 (Fig. 1). Bright-field TEM images of two different regions of the vein are illustrated in (a) and (b), showing localized high strain contrast in the vein-filling apatite with respect to host apatite. The vein consists of an overgrowth of fluorapatite on the host apatite. Insets of selected area electron diffraction (SAED) patterns of host apatite in (a) ([011] zone axis) and apatite in the vein in (b) ([011] zone axis) indicate that the compositionally distinct apatites are in crystallographic continuity. Dark-field STEM images of the vein are shown in (c) and (d), revealing the compositional heterogeneity and a complex nanoporosity in the filled parts of the vein.

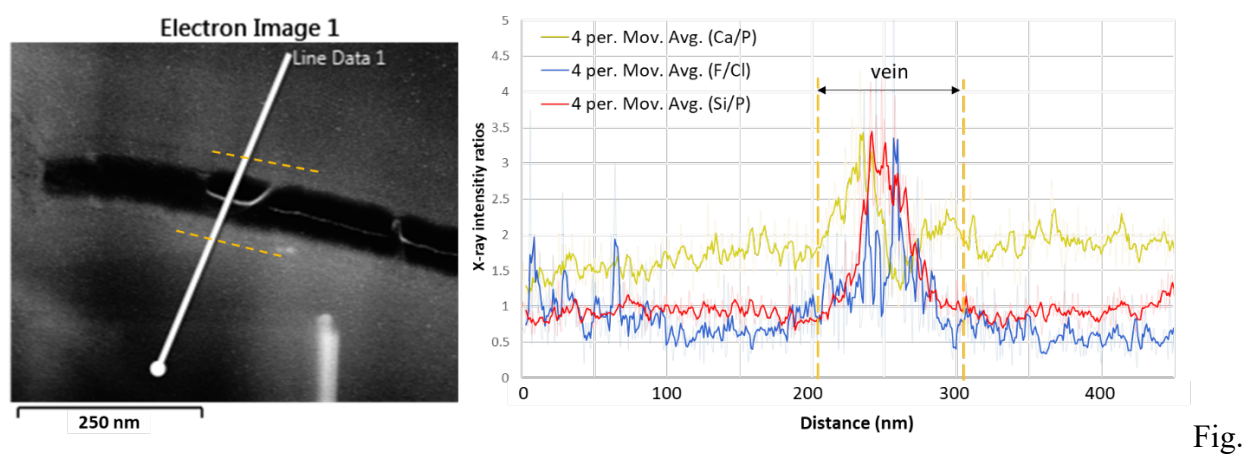


Figure 4. Scanning TEM-EDS X-ray intensity line profile of Ca/P, F/Cl, and Si/P ratios plotted against distance across the apatite NWA 998 vein. The dashed orange lines mark the sharp contact between the vein and the host apatite. The vein in this area is about 100 nm in width. The plot shows the averaged moving trendline every 4 data points to better illustrate the ratios. The F/Cl ratio (blue line) is variable across the vein but overall, F in the vein significantly increases with respect to the host apatite. The Si/P ratio (red line) increases consistently through the vein, and Ca/P ratio although variable, also increases (yellow line).

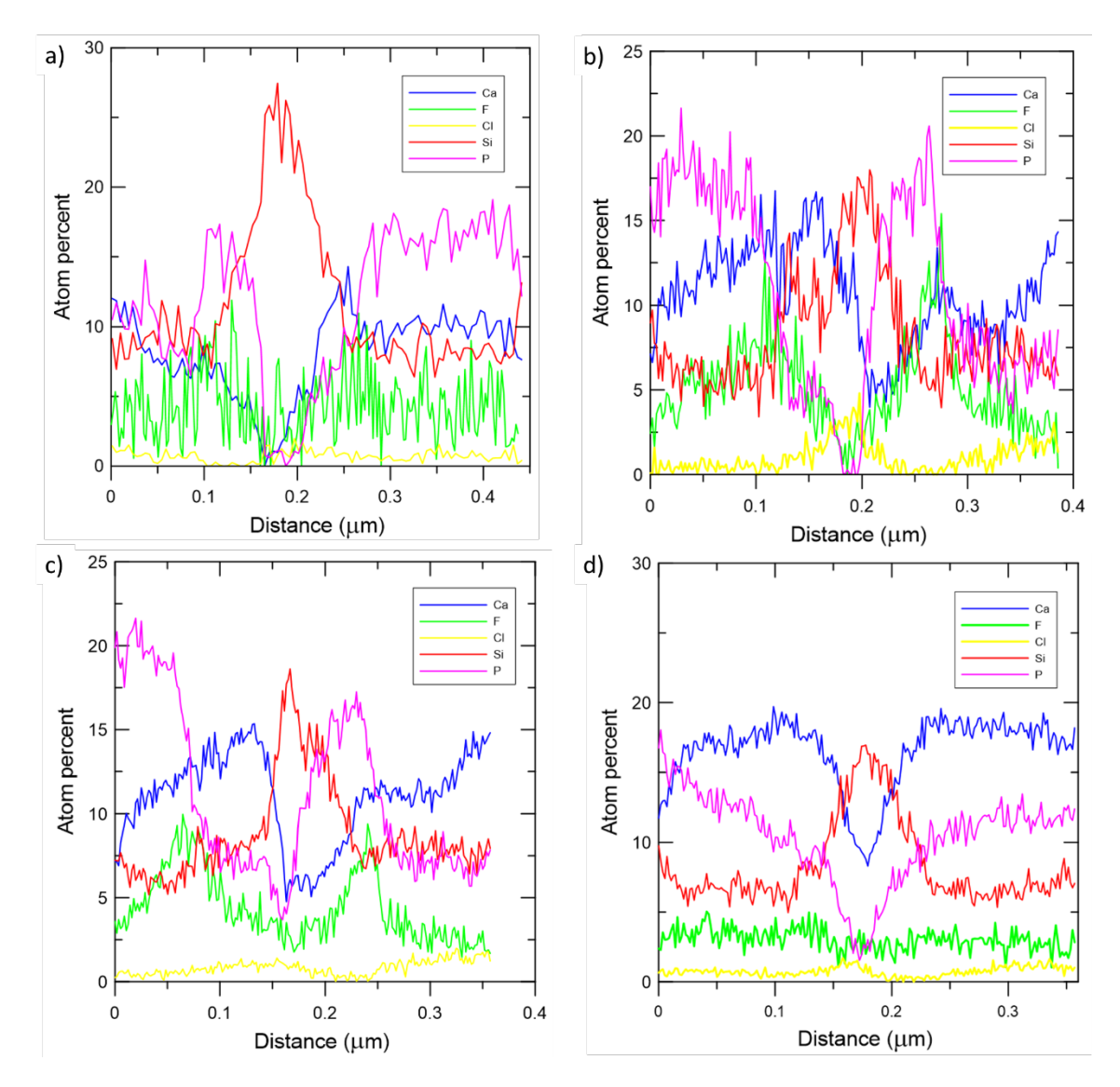


Figure 5. Scanning TEM-EDS X-ray intensity line profiles for Ca, O, F, Cl, Si, and P (atom%) plotted against distance (µm) in different regions across the vein in NWA 998 host apatite.

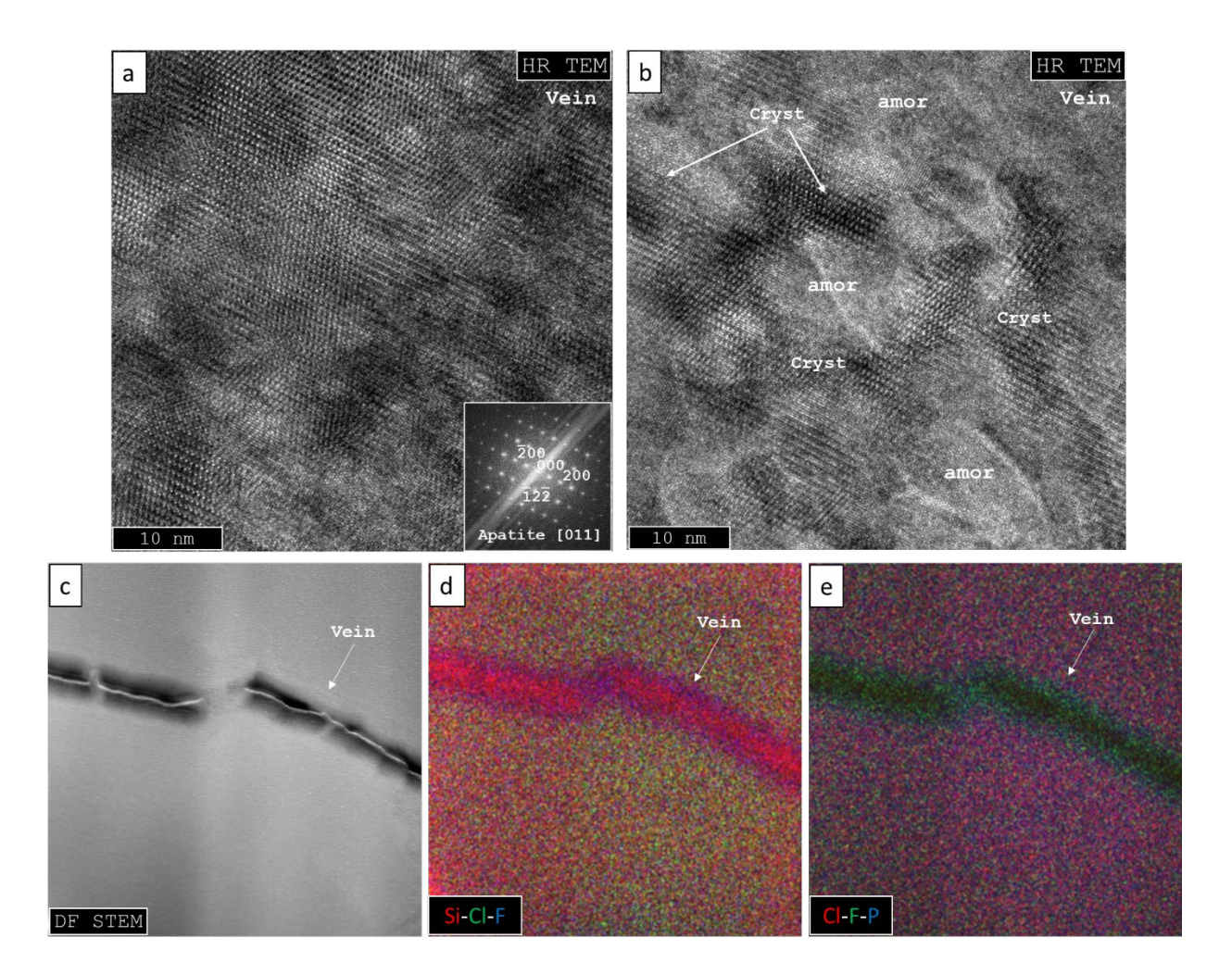


Figure 6. High-resolution TEM and elemental X-ray mapping in the vein of NWA 998 apatite. High-resolution TEM images show crystalline regions with 5-10 nm domains (a) mingled with regions of amorphous material (b). c-e) Dark-field STEM image along with RGB compositional X-ray maps in Si-Cl-F (d) and Cl-F-P (e) show that apatite in the vein is enriched in F on the sides and Si in the center. Abbreviations: amor = amorphous material, Cryst = crystalline apatite.

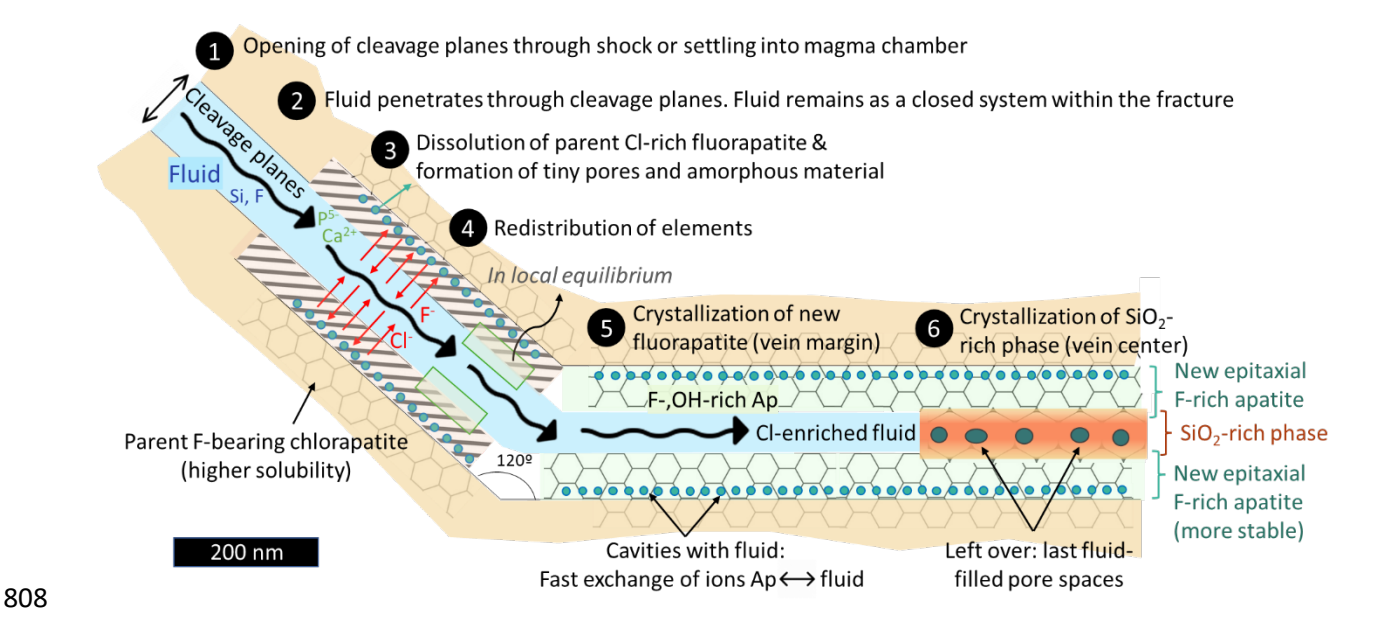


Figure 7. Illustration showing the interface-coupled dissolution-reprecipitation process in the formation of the vein within the cleavage planes of F-bearing chlorapatite in NWA 998. The fluid penetrated the opened cleavage planes producing new epitaxial fluorapatite as at the margins from dissolution of host F-bearing chlorapatite. Steps represented with numbers: (1) opening of cleavage planes, (2) penetration of a F-,Si-rich fluid, (3) dissolution of host F-bearing chlorapatite and formation of tiny pores at the reaction interface, (4) Ca, P, and F go into solution and reprecipitate to form new apatite, (5) Si and possibly F are externally introduced from the fluid, F and OH are preferentially used to form new apatite while the fluid gets enriched in Cl, and finally, (6) crystallization of a silica-rich phase in the vein center.

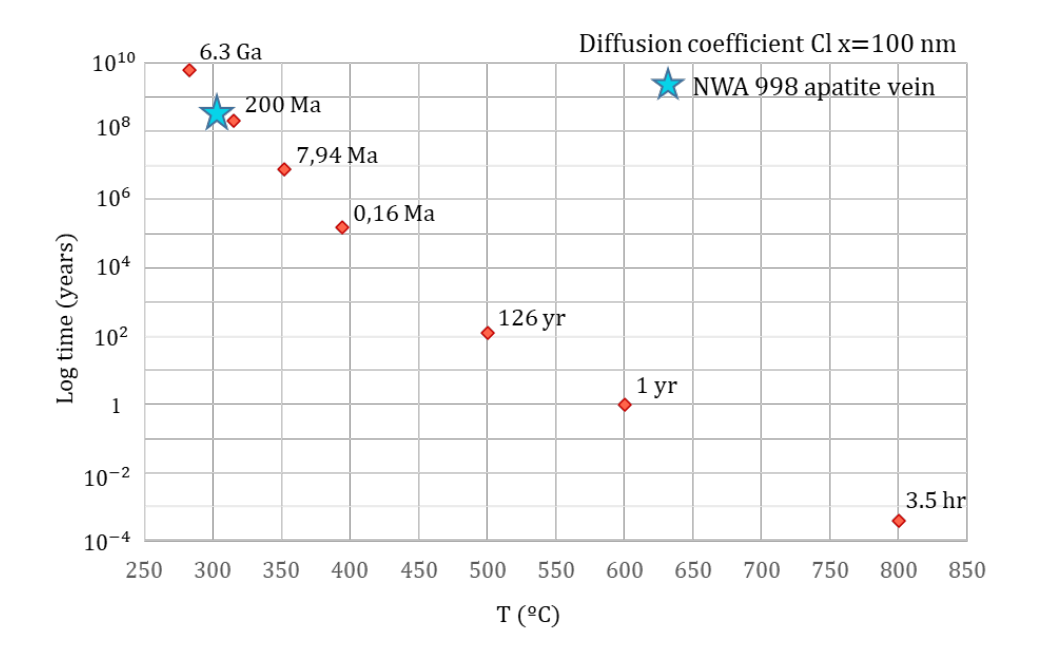


Figure 8. Logarithm of time (years) versus temperature (°C) using different diffusion coefficients of Cl as a function of temperature extracted from Li et al. (2020) (equation 1) and applied to equation 2. The only diffusion coefficient that has been directly extracted from Li et al. (2020) is at 800 °C (3.5 hours). Below 800 °C, diffusion coefficients have been extrapolated.

Table 1. Comparison of S/TEM-EDS analyses (oxide wt%) of the host apatite and apatite plus a Si-rich phase in the vein. Host apatite data extracted from Martínez et al. (2023a).

| Oxides wt% | Host Ap | vein | | |
|-------------------------------------|---------|-------|--|--|
| P_2O_5 | 39.80 | 35.39 | | |
| SiO_2 | 1.98 | 10.4 | | |
| Al_2O_3 | 0.80 | 0.12 | | |
| SO_3 | 0.00 | 0.5 | | |
| CaO | 52.48 | 49.25 | | |
| FeO | 0.36 | 0.24 | | |
| F | 1.48 | 2.96 | | |
| Cl | 3.10 | 1.14 | | |
| Total | 100 | 100 | | |
| Cl/F (wt%) | 2.11 | 0.39 | | |
| Structural formulae based on 13 [O] | | | | |
| P | 2.88 | 2.5 | | |
| Si | 0.17 | 0.87 | | |
| Al | 0.08 | 0.01 | | |
| S | 0.00 | 0.09 | | |
| Ca | 4.81 | 4.4 | | |
| Fe | 0.02 | 0.02 | | |
| F | 0.40 | 0.78 | | |
| Cl | 0.45 | 0.16 | | |
| Z | 0.15 | 0.06 | | |
| Total cat | 7.97 | 7.88 | | |
| Ca/P atomic | 1.67 | 1.76 | | |

n.d. = not detected

Z = missing component (OH + vacancies)